Toughened Epoxy Hybrid Nanocomposites Containing Both an Organophilic Layered Silicate Filler and a Compatibilized Liquid Rubber

Jörg Fröhlich, Ralf Thomann, and Rolf Mülhaupt*

Freiburger Materialforschungszentrum und Institut für Makromolekulare Chemie der Albert-Ludwigs Universität, Stefan-Meier-Str. 31, 79104 Freiburg, Germany

Received July 16, 2003; Revised Manuscript Received July 30, 2003

ABSTRACT: Hexahydrophthalic acid anhydride-cured bisphenol A diglycidyl ether (BADGE) was used as matrix material for hybrid nanocomposites containing both inorganic nanofiller and compatibilized polyether liquid rubbers. Compatibility between organophilic fluorohectorite, modified by means of intergallery cation exchange with bis(2-hydroxyethyl)methyldodecylammonium, and the liquid rubber triol was achieved by partial transesterification of the polyether end groups with methyl stearate to incorporate stearate end groups. Thermal analysis, dynamic mechanical analysis, mechanical testing, wide-angle X-ray scattering, and transmission electron microscopy were used to measure thermal, mechanical, and morphological properties of the hybrid nanocomposites. Without compatibilization, the rubber does not phase separate and flexibilizes the epoxy resin. Toughness is enhanced at the expense of stiffness, strength, and glass temperature. The stearate compatibilizer is sufficient to achieve phase separation of the rubber. This compatibility matching represents the key to novel phase-separated nanocomposites with significantly improved toughness and only marginally lower stiffness.

Introduction

Epoxy resins are thermosets exhibiting an attractive combination of stiffness, strength, high heat distortion temperature, thermal and environmental stability, and creep resistance. They are widely applied as binders of coatings, adhesives, and composites. Frequently, crosslinking is accompanied by embrittlement causing mechanical failure upon straining and impact. It is an important objective to explore new routes toward toughening of epoxy resins without affecting stiffness, strength, and glass temperature.[1]

Since the pioneering advances of B.F. Goodrich researchers during the 1970s, the incorporation of liquid rubbers is used extensively to improve toughness/stiffness balance of thermosets.[2] Several requirements must be met in the development of toughening agents: solubility in the uncured resin without massive increase of solution viscosity and phase separation during cure. The compatibility between liquid rubber and resin must be matched carefully in order to achieve phase separation during cure and simultaneously provide adequate interfacial adhesion.[3] The phase-separated rubber particles are presumed to act as stress concentrators initiating energy absorbing "toughening" processes. According to the literature, the most common micromechanical processes responsible for the increase in fracture toughness are localized shear yielding of the epoxy matrix, plastic void growth in the matrix, which is initiated by cavitation or debonding of the rubber particles, and rubber particle bridging behind the crack tip.[4,5]

Since the early advances of McGarry and the researchers at B.F. Goordrich, compatibility matching has been achieved by varying molecular architectures and reactive end groups of liquid rubbers, such as butadiene−acrylonitrile copolymers containing carboxyl (CTBN), amine (ATBN), or epoxy (ETBN) reactive end groups.[6,7] Other elastomeric modifiers that have been studied include acrylate elastomers[8] and polysiloxanes.[9] Liquid polyethers like poly(propylene oxide)[10−12] or poly(tetrahydrofuran)[13,14] have also been used as toughening agents. Modification of their end groups in order to tailor phase separation behavior and adhesion to the matrix via chemical bonds can easily be achieved. The improvement of fracture toughness by the addition of liquid rubber modifiers, however, is frequently associated with softening of the matrix due to matrix flexibilization. This is not unexpected since the modulus of the modifier is much lower than the modulus of the matrix.

Nanocomposite technology using organophilic layered silicates as in-situ route to nanoreinforcement offers new opportunities for the modification of thermoset micromechanics. Large improvements of mechanical and physical properties including modulus,[15] barrier properties,[16] flammability resistance,[17] and ablation performance[18] have been reported for this type of material at low silicate content. In principle, it should be possible to compensate matrix flexibilization via matrix reinforcement using organophilic layered silicates.

Polymer/layered silicate nanocomposites were first developed by researchers from Toyota based on the thermoplastic polyamide 6[19] and have been extended to thermosets by Giannelis and Pinnavaia.[20,21] Polymer/layered silicate composites are usually divided into three general types: conventional composite with the silicate acting as a filler on the microscale, intercalated nanocomposite based on the insertion of polymer in between the silicate layers which remain in a long-range order, and exfoliated nanocomposite in which individual layers are dispersed in the matrix. Only few attempts have been made so far to combine liquid rubbers and layered silicates to achieve hybrid nanocomposites.[22−24] Particulate inorganic fillers, however, have been extensively

* Corresponding author: e-mail rolf.muelhaupt@makro.uni-freiburg.de.

10.1021/ma035004d CCC: $25.00 © 2003 American Chemical Society
Published on Web 08/20/2003

used in combination with liquid rubbers to enhance the mechanical properties of epoxy resins and other polymeric matrices in industry. Therefore, mainly patents are dealing with these organic/inorganic formulations.[25−28] Another family of epoxy hybrid composites are materials containing both glass beads and liquid rubbers.[29,30]

The objective of this research was to investigate the role of liquid rubber compatibility with organophilic layered silicates in order to achieve simultaneous dispersion of rubber and nanofiller phases. Hexahydrophthalic acid anhydride-cured bisphenol A diglycidyl ether (BADGE) was used as epoxy matrix material for the preparation of hybrid nanocomposites containing organophilic synthetic fluorohectorite, modified by means of interlayer cation exchange of sodium for bis(2-hydroxyethyl)methyldodecylammonium, and liquid trihydroxy-terminated poly(propylene oxide-*block*-ethylene oxide) (PPO) as liquid rubber. Compatibility between liquid rubber and nanofiller as well as between liquid rubber and epoxy resin was varied by transesterification of an average of 20% of the PPO end groups with methyl stearate, thus producing a stearate-functional PPO. Dynamic mechanical analysis (DMA), mechanical testing, wide-angle X-ray scattering (WAXS), and transmission electron microscopy (TEM) were used to examine thermal, mechanical, and morphological properties of hybrid nanocomposites as a function of matching the filler/rubber and rubber/matrix compatibilities.

Experimental Section

Materials. Bisphenol A diglycidyl ether (BADGE, Araldite CY225) and hexahydrophthalic acid anhydride (Hardener HY925) were received from Vantico AG, Switzerland. The hardener HY925 was preaccelerated by a small amount of dimethylbenzylamine. Synthetic fluorohectorite (Somasif ME-100) was supplied by UnicoopJapan Ltd., Japan. Bis(2-hydroxyethyl)methyldodecylammonium chloride (BHEMDA), commercially available from Akzo Nobel Chemicals GmbH, Germany, under the trade name Ethoquad/C12, was employed to render the layered silicate organophilic. The liquid rubber used was a tristar poly(propylene oxide-*block*-ethylene oxide) (PPO) by Bayer AG, Germany (Desmophen VP PU 21IK01, molar mass of 4800 g/mol). End-tipping with ethylene oxide provided primary hydroxy end groups for the PPO. Stearic acid and methyl stearate as well as triphenylphosphane and dibutyltin dilaurate were purchased from Sigma-Aldrich and used as received.

Organosilicate Preparation. The organosilicate Somasif/BHEMDA used in this study was prepared by ion-exchange reaction of Somasif-ME100 with bis(2-hydroxyethyl)methyldodecylammonium chloride (BHEMDA) in aqueous phase as reported elsewhere.[31] The organic content of the organosilicates was recorded using thermogravimetric analysis (TGA) from 30 to 700 °C with a heating rate of 10 K/min under nitrogen.

Modification of Liquid Rubber and Epoxy Resin. To provide the PPO triol liquid rubber with stearate end groups, 1503 g of poly(propylene oxide-*block*-ethylene oxide) (0.31 mol of PPO, 0.93 mol of OH) was first dried in a round-bottom flask for 1 h at 100 °C at 0.1 hPa pressure. Then, 56 g of methyl stearate (0.19 mol, an equivalent of 20% regarding the hydroxy end groups of the PPO) and 7.1 mL of dibutyltin dilaurate (7.7 g, 0.5 wt %) as a catalyst were added. The mixture was heated to 160 °C and was stirred for 70 h under continuous nitrogen flow. Afterward, a vacuum of 0.1 hPa was used to degass the slightly yellow product and remove traces of methyl stearate and methanol, the latter being formed during the reaction.

The epoxy resin was modified via addition of stearic acid. Therefore, 2000 g of BADGE (Araldite CY225) (5.3 mol) was heated to 80 °C in a round-bottom flask under an argon atmosphere, and 53 g of stearic acid (0.19 mol, 3.5% regarding BADGE) and 243 mg of triphenylphosphane (0.5 mol % regarding carboxylic groups) as a catalyst were added. After stirring the mixture for 5 h at 80 °C, a slightly yellow viscous liquid was obtained. This modified epoxy resin was used in the preparation of some hybrid nanocomposites instead of the pristine Araldite CY225. The products of both modification reactions were examined using a 300 MHz spectrometer for proton NMR analysis in deuteriochloroform.

Epoxy Hybrid Nanocomposite Preparation. Somasif/BHEMDA was thoroughly mixed for 8 h at 60 °C with different amounts of PPO, either unmodified or bearing stearate moieties, using a Molteni Planimax high shear mixer to obtain additive master batches containing 67 or 90 wt % of liquid rubber, respectively.

Sixty grams of each additive master batch was mixed with 300 g of bisphenol A diglycidyl ether (Araldite CY225) at 80 °C and 10 hPa pressure for the duration of 45 min with a Molteni Planimax high shear mixer in order to achieve dispersion and to reduce residual water. Then, 240 g of hexahydrophthalic acid anhydride (Hardener HY925) was added, and the mixture was stirred at 80 °C and 10 hPa for another 30 min. The resin was then poured into a mold (200 × 200 × 4 mm^3), and curing was performed at 140 °C for 14 h in a vented oven to produce epoxy hybrid nanocomposites containing 10 wt % of hybrid additive. All different hybrid nanocomposites containing 5, 10, or 15 wt % of additive were produced according to this method. In the case of the modified epoxy resins, the BADGE bearing stearate chains was used instead of the pristine Araldite CY225. Additionally, composites containing only one additive component, either organosilicate (2.5−7.5 wt %) or PPO (5−15 wt %), were also prepared for comparison purposes. Characterization by means of WAXS, TEM, and mechanical testing was conducted as reported elsewhere.[32]

Dynamic Mechanical Analysis. Specimens with a dimension of 50 × 4 × 2.5 mm^3 were measured by means of temperature sweeps from −100 to 180 °C in a Rheometrics dynamic mechanical analyzer RSA II equipped with dual cantilever geometry at a frequency of 0.3 Hz, a strain of 0.08%, and a scanning rate of 2 K/min.

Results and Discussion

Hybrid Nanocomposite Preparation. To prepare the epoxy hybrid nanocomposites, the organophilic flouorhectorite modified with bis(2-hydroxyethyl)methyldodecylammonium (BHEMDA) was first blended toegther with tristar poly(propylene oxide-*block*-ethylene oxide) (PPO) liquid rubber, thus producing a master batch paste containing 90 or 67 wt % PPO, respectively. These different pastes were added to an epoxy resin consisting of bisphenol A diglycidyl ether (BADGE) and hexahydrophthalic acid anhydride in amounts varying from 5 and 10 wt % to 15 wt %. All of the final blends possessed viscosities in the range of the neat epoxy system, thus retaining good processability. The compatibility between PPO liquid rubber and organophilic fluorohectorite was varied by transesterification of 20% of the PPO hydroxy end groups with methyl stearate to produce stearate-functionalized PPO as compatibilized liquid rubber. Formation of a BADGE adduct with 3.5 wt % stearic acid was used to improve compatibility between the organohectorite and the epoxy matrix.

Three series of hybrid nanocomposites were prepared using (1) unmodified PPO liquid rubbert or (2) stearate-modified PPO liquid rubber, both in combination with fluorohectorite modified with BHEMDA, in virgin epoxy resin (called "ER-PPO" and "ER-PPO-stearate", respectively), and (3) unmodified PPO triol and organophilic fluorohectorite in stearate-modified epoxy resin (called "ER-PPO + adduct"). Within each series, the liquid rubber content of the additive employed was held

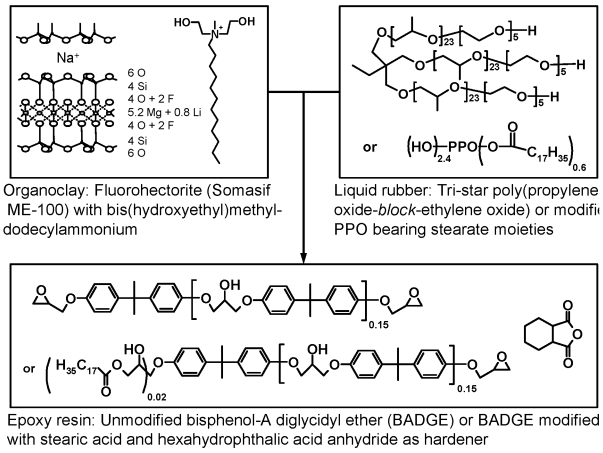

Figure 1. Materials and reaction scheme of the preparation of hybrid nanocomposites containing organophilic layered silicate and liquid rubber.

constant at either 90 or 67 wt %, signified by the first number in the sample's name. The various components and an overview of the preparation of the epoxy hybrid nanocomposites are displayed in Figure 1.

Composites containing only one of the components of the hybrid systems, organophilic fluorohectorite or PPO alone (called "ER-PPO" or "ER-BHEMDA"), were also prepared for comparison. When incorporating the organophilic fluorohectorite Somasif/BHEMDA alone, loadings of 2.5−7.5 wt % were chosen to be comparable to the organosilicate content of the hybrid nanocomposites. Compositions of all epoxy resins made are listed in Table 1. The calculation of the true silicate content in Table 1 is based on the results of the TGA of the organohectorite Somasif/BHEMDA. Heated up to 700 °C it shows a weight loss of 23.8%, signifying a silicate content of 76.2%. Thus, the loading of the layered silicate with BHEMDA is 97 mequiv/100 g, which is in good agreement with the ion exchange capacity of 100 mequiv/100 g reported for Somasif ME-100 (supplier data).

Morphology. Wide-angle X-ray scattering (WAXS) was employed during all stages of the hybrid nanocomposite preparation to monitor the changes in the silicate's interlayer distances. The results are summarized in Table 2. Because of the organophilic modification of Somasif ME-100 with bis(2-hydroxyethyl)methyldodecylammonium, the interlayer distance increased from 0.94 nm in the neat fluorohectorite to 2.32 nm in the organophilic fluorohectorite. During mixing of the organophilic flouorohectorite with unmodified PPO, the layered silicate interlayer distance was expanded to 3.39 nm, whereas the addition of stearate-modified PPO afforded interlayer distances of 2.39 nm. The altered polarity of the stearate-modified PPO renders the polymer less compatible with the organohectorite so that the intercalation of the silicate layers with the liquid rubber is less favored.

After curing of the epoxy resin, the hybrid nanocomposite containing PPO-stearate shows a slight increase of the interlayer distance from 2.39 to 2.94 nm due to epoxy polymerization between the silicate layers. The same interlayer distance is observed in the nanocomposite with Somasif/BHEMDA as the only additive. Hence, the use of PPO-stearate does not deteriorate the intercalation of the silicate layers. On the other hand, in the composites containing unmodified PPO, the interlayer distance is significantly enlarged during epoxy polymerization. In the WAXS diagram a broad band and no distinct peak is visible at low angles, indicating a wide distribution of different distances. Transmission electron microscopy (TEM, see below) shows, however, that the single silicate layers are still stacked remaining in a certain short-range order instead of being fully exfoliated.

In contrast, the silicate interlayer distance in the hybrid nanocomposite prepared with stearate-modified BADGE decreases to 2.85 nm during epoxy cure. Most likely, the PPO is leaving the interlayer galleries being dissolved in the modified BADGE. A superior compatibility between the PPO and the modified epoxy resin in comparison to the galleries of the Somasif/BHEMDA might be the reason for the collapse of the silicate layers. Thus, the stearate modification of the epoxy resin did not result in an improved exfoliation of the organosilicate in the hybrid material. As shown above, the unmodified PPO in the additive mixture, on the other

Table 1. Compositions of the Epoxy Hybrid Nanocomposites Containing Organohectorite Somasif/ BHEMDA and PPO Triol Liquid Rubber

sample	additive loading (wt %)	organo-silicate content (wt %)	true silicate content (wt %)	PPO content (wt %)
Epoxy Resin (Unmodified)				
ER-0	0	0	0	0
With Somasif/BHEMDA				
ER-BHEMDA/2,5	2.5	2.5	1.9	0
ER-BHEMDA/5	5	5	3.8	0
ER-BHEMDA/7,5	7.5	7.5	5.7	0
With PPO				
ER-100PPO/5	5	0	0	5
ER-100PPO/10	10	0	0	10
ER-100PPO/15	15	0	0	15
(1) With PPO and Somasif/BHEMDA				
ER-90PPO/5	5	0.50	0.4	4.50
ER-90PPO/10	10	1.00	0.8	9.00
ER-90PPO/15	15	1.50	1.1	13.50
ER-67PPO/5	5	1.67	1.3	3.33
ER-67PPO/10	10	3.33	2.5	6.67
ER-67PPO/15	15	5.00	3.8	10.00
(2) With PPO-Stearate and Somasif/BHEMDA				
ER-90PPO-stearate/5	5	0.50	0.38	4.50
ER-90PPO-stearate/10	10	1.00	0.76	9.00
ER-90PPO-stearate/15	15	1.50	1.14	13.50
ER-67PPO-stearate/5	5	1.67	1.27	3.33
ER-67PPO-stearate/10	10	3.33	2.54	6.67
ER-67PPO-stearate/15	15	5.00	3.81	10.00
(3) BADGE-Adduct with PPO and Somasif/BHEMDA				
ER-90PPO+adduct/5	5	0.50	0.38	4.50
ER-90PPO+adduct/10	10	1.00	0.76	9.00
ER-90PPO+adduct/15	15	1.50	1.14	13.50
ER-67PPO+adduct/5	5	1.67	1.27	3.33
ER-67PPO+adduct/10	10	3.33	2.54	6.67
ER-67PPO+adduct/15	15	5.00	3.81	10.00

Table 2. Interlayer Distances of the Organohectorite, the Different Additive Master Batches, and the Therewith Prepared Epoxy Hybrid Nanocomposites Determined by WAXS

sample	interlayer distance (nm)
Somasif ME−100	0.94
Somasif BHEMDA	2.32
ER-BHEMDA/10	2.94
67PPO	3.39
ER-67PPO/10	no peak
ER-67PPO + adduct/10	2.85
67PPO-stearate	2.39
ER-67PPO-stearate/10	2.94

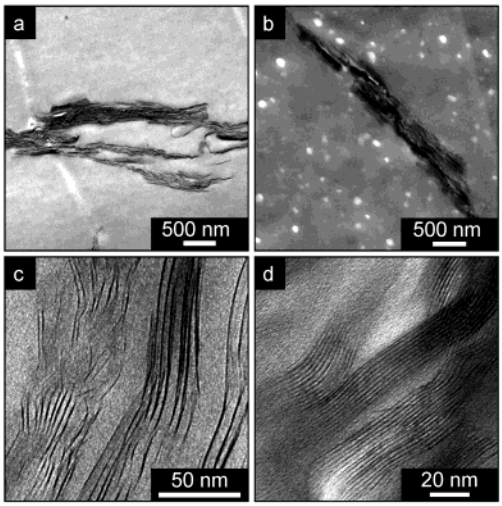

Figure 2. Transmission electron micrographs of epoxy hybrid nanocomposites. Images shown are examples for composites with (a) dissolved PPO (ER-67PPO + adduct/15) and (b) phase-separated PPO-stearate spheres (ER-90PPO-stearate/10) in the epoxy matrix. Image (c) depicts intercalated silicate layers with different interlayer distances in a PPO-modified composite (ER-67PPO/15), whereas the composite containing PPO-stearate (ER-90PPO-stearate/10) exhibits intercalated layers in a long-range order (d).

hand, eases the diffusion of BADGE molecules between the silicate layers during cure leading to an intercalated morphology with large interlayer distances. These results confirm the importance of the compatibility between epoxy resin and organosilicate as a prerequisite for interlayer polymerization and the preparation of exfoliated nanocomposites, as suggested by Pinnavaia et al.[33]

The transmission electron micrographs in Figure 2 illustrate the different morphologies present in the hybrid nanocomposites depending on formulation. Composites containing unmodified PPO, either formulated with unmodified BADGE or stearate-modified BADGE, possess a homogeneous matrix with dispersed silicate particles on a microscale (a). The silicate particles in the PPO-stearate hybrid nanocomposites are similarly dispersed in the matrix. The striking difference between these two types of composites is, however, the phase-separated morphology of the rubber particles in the PPO-stearate composite (b). Because of the altered polarity of the stearate-modified PPO, the liquid rubber phase-separates during cure forming randomly dispersed particles. Small spheres with diameters of 50−200 nm are developed in the matrix, whereas the unmodified PPO stays dissolved in the epoxy resin even after completion of cure. TEM examinations of all samples indicate that the PPO-stearate forms dispersed particles only in the hybrid composites with liquid rubber contents exceeding about 9 wt %: ER-90PPO-stearate/10, ER-90PPO-stearate/15, and ER-67PPO-stearate/15 (containing 9, 13.5, and 10 wt % liquid rubber, respectively). Samples with lower loadings show a homogeneous matrix, pointing at a limited solubility of the PPO-stearate in the epoxy matrix. When being observed visually, nanocomposites comprising miscible PPO were translucent, whereas the PPO-stearate blends with separated particles were opaque.

As illustrated by WAXS, smaller but also visible differences between the hybrid nanocomposites containing either pure PPO or PPO-stearate exist on the nanoscale. The PPO-stearate hybrid composites show less extended interlayer distances and almost evenly spaced silicate layers (image d), yielding sharp WAXS peaks (see above). The layered silicates dispersed in the materials containing unmodified PPO liquid rubber, however, possess larger interlayer spacing, and the single layers are not regularly ordered (image c). Thus, no WAXS peak could be detected for the samples with unmodified PPO. All hybrid nanocomposites are, however, still only intercalated. Exfoliation of layered silicates via in-situ polymerization of thermosets is generally hard to achieve due to the fact that the ongoing network formation outside the silicate particles locks the layers within a long-range order.

Dynamic Mechanical Properties. DMA measurements of the hybrid nanocomposites gave lowered glass transition temperatures (T_g) for all samples. The values of T_g vary between 100 and 110 °C for the composite materials compared to 127 °C for the neat resin. In general, the T_g of the materials decreases with increasing additive loading and hence amount of liquid rubber. Even the T_g of the nanocomposites containing only Somasif/BHEMDA, and no PPO are slightly lowered compared to the neat resin. Table 3 lists the T_g values of all samples.

Figure 3 illustrates the differences in the dynamic mechanical properties of the different hybrid nanocomposite formulations. As mentioned above, the glass transition temperatures of the composites are lowered compared to the neat resin because liquid rubber is dissolved in the epoxy matrix. Moreover, the addition of PPO and layered silicate might modify the anhydride cure of the epoxy resin and affect the final network properties. For example, hydroxy end groups of the PPO can react with anhydride hardener, forming ester linkages and acid groups. Furthermore, the alkylammonium cations used to modify the layered silicate are known to catalyze epoxy homopolymerization unbalancing the stoichiometry of resin and hardener. Even traces of the DBTDL, used as a catalyst for the preparation of the PPO-stearate, might interfere with the epoxy anhydride reaction.

However, a typical order in T_g values—as represented for one series of formulations in Figure 3—can be elucidated out of all data: The T_g of the PPO-stearate composite is slightly higher than that of the other composite materials because of its phase-separated morphology and therefore smaller quantities of liquid rubber dissolved in the matrix. Because of the stearate modification of the BADGE, which reduces network density and increases PPO solubility, the PPO + adduct hybrid nanocomposites possess the lowest glass transition temperatures. The flexural modulus of the hybrid materials shows a similar dependence on temperature as the neat resin. Thus, the stiffness, even at elevated temperatures, is not severely affected by the additives. The loss factor tan δ at lower temperatures, however, differs for the various composites. In all samples a β-relaxation of the epoxy network was measured to occur around −90 °C. The hybrid nanocomposites containing unmodified PPO liquid rubber show another broad band at about −50 °C. This weak, but individual, signal of the glass transition of the liquid rubber indicates an incomplete phase separation, although the matrix seems to be homogeneous in the transmission electron micrographs. The DMA curve of the PPO-stearate composite confirms the phase-separated mor-

Table 3. Glass Transition Temperatures and Mechanical Properties of Epoxy Hybrid Nanocomposites Determined by DMA and Tensile Testing

sample	T_g (°C)	tensile modulus (MPa)	yield strength (MPa)	elongation at break (%)	K_{Ic} (MPa m$^{1/2}$)
ER-0	127	3390	79	8.2	0.67
ER-BHEMDA/2,5	123	3360	40	1.3	0.96
ER-BHEMDA/5	123	3500	43	1.3	1.07
ER-BHEMDA/7,5	122	3620	42	1.3	1.23
ER-100PPO/5	116	2890	71	6.9	0.98
ER-100PPO/10	110	2440	54	9.0	1.37
ER-100PPO/15	105	1980	41	10.5	1.28
ER-90PPO/5	114	2980	71	6.0	1.27
ER-90PPO/10	105	2620	60	5.8	1.33
ER-90PPO/15	100	2230	50	6.9	1.18
ER-67PPO/5	112	3320	50	1.7	1.33
ER-67PPO/10	109	3120	41	1.4	1.37
ER-67PPO/15	106	2860	38	1.5	1.41
ER-90PPO-stearate/5	114	3060	77	4.0	1.33
ER-90PPO-stearate/10	110	2740	66	4.0	1.69
ER-90PPO-stearate/15	106	2420	52	4.6	2.48
ER-67PPO-stearate/5	112	3370	41	1.3	1.36
ER-67PPO-stearate/10	110	3230	39	1.3	1.83
ER-67PPO-stearate/15	109	3010	32	1.2	1.74
ER-90PPO+adduct/5	111	3020	77	5.7	1.08
ER-90PPO+adduct/10	104	2660	66	4.6	1.12
ER-90PPO+adduct/15	99	2200	48	7.4	1.28
ER-67PPO+adduct/5	110	3330	40	1.3	1.12
ER-67PPO+adduct/10	104	3150	38	1.3	1.18
ER-67PPO+adduct/15	102	2890	32	1.2	1.46

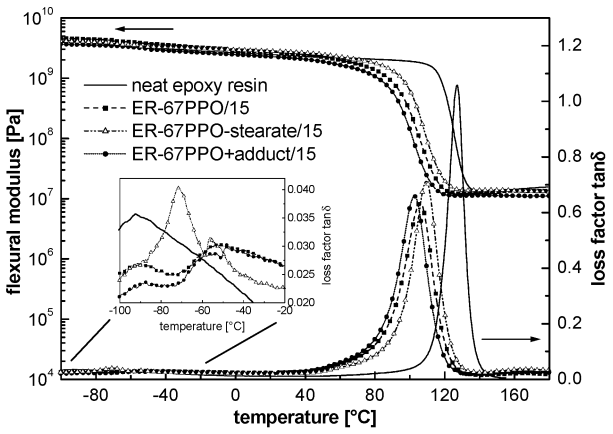

Figure 3. DMA diagrams of various epoxy hybrid nanocomposites with additive loadings of 15 wt % in comparison to the neat epoxy resin. The inset shows the loss factor between −100 and −20 °C in greater detail.

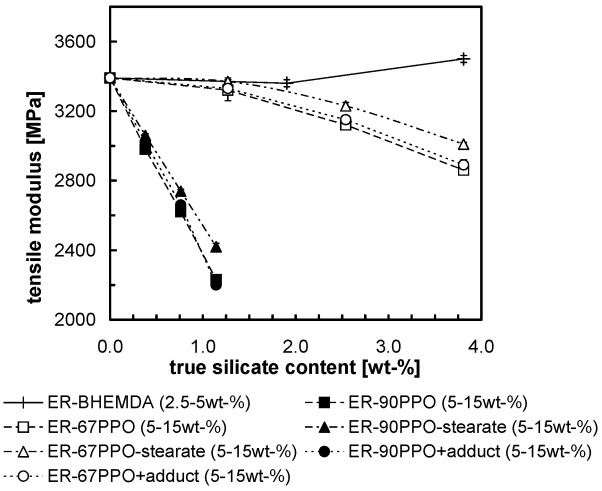

Figure 4. Evolution of the tensile modulus of the different hybrid nanocomposites filled with true silicate content. The epoxy resin with the organohectorite Somasif/BHEMDA alone is included for comparison.

phology observed by TEM in showing a distinct peak at −70 °C. The lower temperature of this relaxation compared to the composite with unmodified PPO can be explained by the lower T_g of the stearate-modified liquid polymer (−67 °C for PPO-stearate compared to −59 °C for pristine PPO according to DSC). Its glass transition is lowered by the incorporation of the nonpolar stearate chains which weaken the intermolecular hydrogen bonds between the PPO.

Mechanical Properties. The mechanical properties of the various hybrid nanocomposites were examined at room temperature by means of tensile testing. Fracture toughness was elucidated in bend-notch geometry. The results for the hybrid materials and the single-component composites (with Somasif/BHEMDA or PPO alone) are listed in Table 3.

The tensile moduli of all hybrid composites are lowered compared to that of the neat epoxy resin. According to Figure 4, the stiffness decreases with increasing additive loading, and the extent highly depends on the amount of silicate in the material. Therefore, the true silicate content of all different samples is used as abscissa for better comparability. With low silicate loadings, implying high PPO contents as in the 90PPO series, the moduli drop by about 30%, regardless of the formulation of the hybrid composites. On the other hand, when the organohectorite content is higher and the PPO content is lower (confer the 67PPO series), the moduli are only decreased by about 10%. For the silicate nanocomposites, though, the moduli slightly increase with increasing silicate content. Thus, the liquid rubber acts as a plastifying agent in the hybrid nanocomposites because of its solubility in the epoxy matrix. Phase separation of PPO-stearate is able to improve the stiffness compared to the materials comprising dissolved pristine PPO.

The decrease in stiffness is accompanied by an increase in toughness for all hybrid nanocomposites. The extent of toughness improvement depends again on the silicate content and additionally on the specific formulation of the various materials. Figure 5 shows the

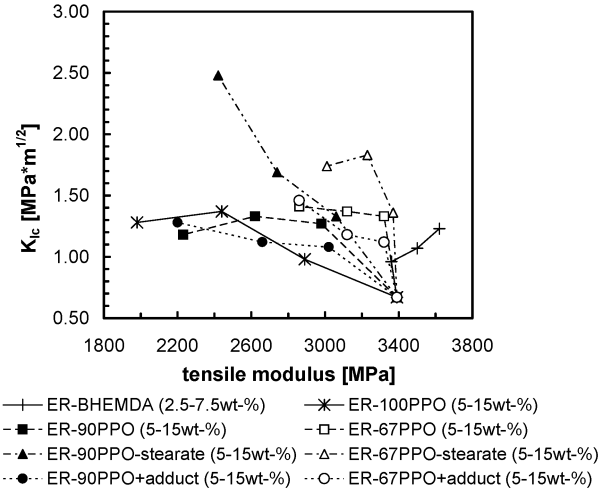

Figure 5. Evolution of the fracture toughness (by means of the stress intensity factor K_{Ic}) of the different hybrid nanocomposites with true silicate content. The epoxy resin containing Somasif/BHEMDA as single filler is included for comparison.

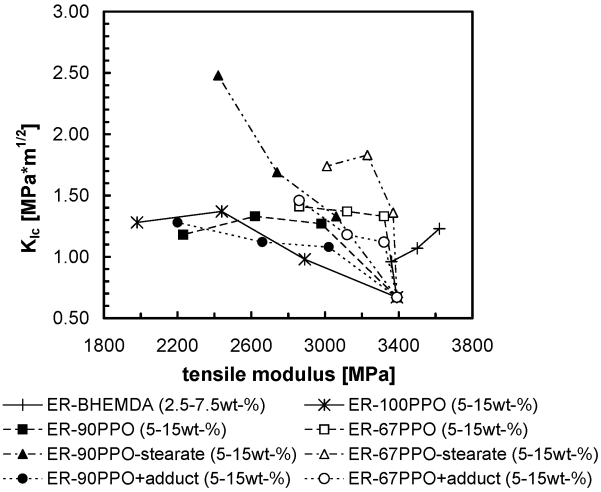

Figure 6. Toughness/stiffness balance of the hybrid nanocomposites. Epoxy resins containing either Somasif/BHEMDA or unmodified PPO alone are included for comparison.

evolution of the fracture toughness K_{Ic} with true silicate content. The values of K_{Ic} can be improved by about 100% when pure PPO is used in combination with organohectorite for hybrid material preparation. This increase in toughness is achieved with low as well as high loadings of silicate. With PPO-stearate as liquid rubber the fracture toughness can be further improved depending on the silicate content. With high organohectorite loadings, the K_{Ic} value experiences a 3-fold increase (from 0.67 to 1.83 MPa m$^{1/2}$ for ER-67PPO-stearate/10), and with lower silicate contents, indicating higher amounts of liquid rubber, the K_{Ic} value can even be enhanced to nearly 400% (2.48 MPa m$^{1/2}$ for ER-90PPO-stearate/15). In contrast, the toughness of the silicate nanocomposites without liquid rubber is only slightly increased with increasing Somasif/BHEMDA content. Hence, the liquid rubber in the hybrid nanocomposites acts as an effective toughness enhancer, especially when a phase-separated morphology has been developed during cure.

The loss of tensile strength encountered for the materials with high silicate loadings is likely due to an inhomogeneous network density. The cure speed of bulk resin and epoxy resin within the silicate galleries may differ, thus causing internal stresses which are responsible for reduced resistance against large mechanical stresses.

Figure 6 shows the toughness/stiffness balance of the hybrid nanocomposites in comparison to composites containing liquid rubber or organohectorite as single modifier. All composites containing unmodified PPO show a moderate increase in toughness combined with a dramatic decrease in stiffness. This decrease in stiffness is more pronounced for higher liquid rubber contents pointing at the PPO's role as plasticizer. The partial modification of BADGE with stearate chains, which lowers network density, deteriorates toughness and stiffness of the materials compared to the composites prepared with unmodified BADGE.

High toughness combined with almost unchanged stiffness compared to the neat resin is achieved when phase-separating PPO-stearate is employed in the hybrid composite preparation. Again, the stiffness of these materials is improved with higher silicate content. According to the toughness/stiffness balance, the hybrid nanocomposites with stearate-modified PPO and higher amount of organosilicate (ER-67PPO-stearate series) offer the best combination of significantly improved toughness and only slightly lowered stiffness. In terms of toughness, these hybrid materials are superior to the organohectorite nanocomposites which combine improved stiffness with only slightly increased toughness.

Conclusions

Epoxy hybrid nanocomposites containing organophilicly modified layered silicates and liquid poly(propylene oxide-*block*-ethylene oxide) were synthesized to combine the different properties which normally result from the use of the single fillers and hence aim at an improved toughness/stiffness balance.

Hexahydrophthalic acid anhydride-cured bisphenol A diglycidyl ether (BADGE) served as the epoxy matrix for additive mixtures of organophilicly modified fluorohectorite and liquid poly(propylene oxide-*block*-ethylene oxide) (PPO). In separate experiments the polarity of either BADGE or PPO was altered by incorporating a small number of stearate as compatibilizer into these compounds. After curing, intercalated nanocomposites with layer distances of about 2.9 nm (measured by WAXS) were obtained. No exfoliation was achieved, not even with the stearate modification of either BADGE or PPO. DMA revealed lowered T_g's of about 110 °C for the hybrid nanocomposites compared to 127 °C of the neat resin. No distinct relaxation peak of the PPO was detected for the corresponding composites. This is due to incomplete phase separation of the liquid polymer upon cure. Only the hybrid nanocomposite containing the stearate-modified PPO showed a distinct relaxation peak, indicating at a phase separation of the PPO because of its lower solubility in the epoxy matrix.

Various morphologies, examined by TEM, arise from the different compatibility of the liquid rubber with the cured epoxy matrix. Hybrid composites containing unmodified PPO or compatibilized BADGE comprise intercalated layered silicates embedded in a homogeneous epoxy matrix in which the PPO is dissolved. This results in a softened nanocomposite with lower stiffness (about 2700 MPa instead of 3300 MPa) and improved toughness (K_{Ic} values of about 1.2 MPa m$^{1/2}$ instead of

0.7 MPa $m^{1/2}$) compared to those of the neat resin. In contrast, if the solubility of the liquid polymer in the cured epoxy is lowered by modification with methyl stearate, a toughened hybrid composite with phase-separated morphology results at higher additive loadings. Spherical polymer particles are formed in the epoxy matrix apart from the silicate particles. The separated polymer phase is then responsible for a major improvement in toughness by 300% compared to the neat resin (up to K_{Ic} values of about 2.0 MPa $m^{1/2}$). The stiffness of these materials is thereby only slightly lowered by 10% (to about 3000 MPa). The design of compatibilized hybrid nanocomposites with compatibilizer-induced phase separation and phase selective filling and modification of interfaces represents a very versatile new tool to enhance the properties of well-established thermoset/rubber and possibly also thermoplastics/rubber blends.

Acknowledgment. The authors gratefully acknowledge financial support by the Sonderforschungsbereich SFB 428 of the Deutsche Forschungsgemeinschaft (DFG). We also thank Dr. Jürgen Finter for his help with the mechanical testing of the hybrid nanocomposites.

References and Notes

(1) May, C. A. *Epoxy Resins*, 2nd ed.; Marcel Dekker: New York, 1988.
(2) Drake, R. *Polym. Mater. Sci. Eng.* **1990**, *63*, 802−805.
(3) Pascault, J.-P. *Macromol. Symp.* **1995**, *93*, 43−51.
(4) Bucknall, C. B. *Toughened Plastics*; Applied Science Publ.: London, 1977.
(5) Pearson, R. A.; Yee, A. F. *J. Mater. Sci.* **1986**, *21*, 2475−2488.
(6) McGarry, F. J.; Willner, A. M. *ACS, Div. Org. Coat. Plast. Chem. Pap.* **1968**, *28*, 512−525.
(7) McGarry, F. J.; Sultan, N. J. *ACS, Div. Org. Coat. Plast. Chem. Pap.* **1968**, *28*, 526−536.
(8) Ratna, D.; Banthia, A. K.; Deb, P. C. *J. Appl. Polym. Sci.* **2000**, *78*, 716−723.
(9) Bauer, R. S., Ed. *Epoxy Resin Chemistry II*; ACS Symposium Series 21; American Chemical Society: Washington, DC, 1984.
(10) Harani, H.; Fellahi, S.; Bakar, M. *J. Appl. Polym. Sci.* **1999**, *71*, 29−38.
(11) Aizpurua, B.; Franco, M.; Corcuera, M. A.; Riccardi, C. C.; Mondragon, I. *J. Appl. Polym. Sci.* **2000**, *76*, 1269−1279.
(12) He, S.; Shi, K.; Bai, J.; Zhang, Z.; Li, L.; Du, Z.; Zhang, B. *Polymer* **2001**, *42*, 9641−9647.
(13) Albert, P.; Läuger, J.; Kressler, J.; Mülhaupt, R. *Acta Polym.* **1995**, *46*, 68−73.
(14) Albert, P.; Läuger, J.; Kressler, J.; Mülhaupt, R. *Acta Polym.* **1995**, *46*, 74−78.
(15) Kojima, Y.; Usuki, A.; Kawasumi, M.; Okada, A.; Fukushima, Y.; Kurauchi, T.; Kamigaito, O. *J. Mater. Res.* **1993**, *8*, 1185−1189.
(16) Yano, K.; Usuki, A.; Okada, A. *J. Polym. Sci., Part A: Polym. Chem.* **1997**, *35*, 2289−2294.
(17) Gilman, J. W.; Kashiwagi, T.; Lichtenhan, J. D. *SAMPE J.* **1997**, *33*, 40−46.
(18) Vaia, R. A.; Price, G.; Ruth, P. N.; Nguyen, H. T.; Lichtenhan, J. D. *Appl. Clay Sci.* **1999**, *15*, 67−92.
(19) Okada, A.; Fukushima, Y.; Kawasumi, M.; Inagaki, S.; Usuki, A.; Sugiyama, S.; Kurauchi, T.; Kamigaito, O. US 4739007, 1988.
(20) Messersmith, P. B.; Giannelis, E. P. *Chem. Mater.* **1994**, *6*, 1719−1725.
(21) Lan, T.; Kaviratna, P. D.; Pinnavaia, T. J. *Chem. Mater.* **1994**, *7*, 2144−2150.
(22) Ivanova, K. I.; Pethrick, R. A.; Affrossman, S. *Polymer* **2000**, *41*, 6787−6796.
(23) Ivanova, K. I.; Pethrick, R. A.; Affrossman, S. *J. Appl. Polym. Sci.* **2001**, *82*, 3468−3476.
(24) Chen, Z.; Gong, K. *J. Appl. Polym. Sci.* **2002**, *84*, 1499−1503.
(25) Kenyon, A. S.; Slocombe, R. J. US 3518221, 1970.
(26) Murphy, W. T.; Guiley, C. D. Jr. US 4320047, 1982.
(27) McGarry, F. J. US 4478963, 1984.
(28) Mülhaupt, R. US 5278257, 1994.
(29) Maxwell, D.; Young, R. J.; Kinloch, A. J. *J. Mater. Sci., Lett.* **1984**, *3*, 9−12.
(30) Kinloch, A. J.; Maxwell, D.; Young, R. J. *J. Mater. Sci.* **1985**, *20*, 4169−4184.
(31) Zilg, C.; Thomann, R.; Finter, J.; Mülhaupt, R. *Macromol. Mater. Eng.* **2000**, *280/281*, 41−46.
(32) Zilg, C.; Mülhaupt, R.; Finter, J. *Macromol. Chem. Phys.* **1999**, *200*, 661−670.
(33) Lan, T.; Kaviratna, P. D.; Pinnavaia, T. J. *J. Mater. Chem.* **1995**, *7*, 2144−2150.

MA035004D